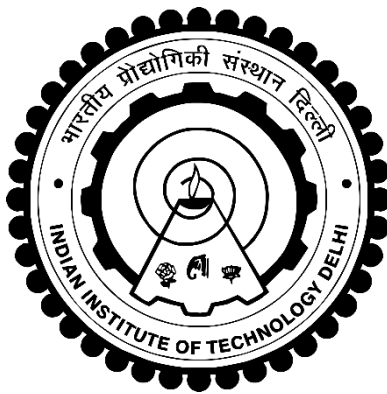


**MODELLING OF NANOSTRUCTURES USING
SECOND-ORDER STRAIN GRADIENT
NONLOCAL THEORY**

BISHWESHWAR BABU



**DEPARTMENT OF APPLIED MECHANICS
INDIAN INSTITUTE OF TECHNOLOGY DELHI
AUGUST 2019**

©Indian Institute of Technology Delhi (IITD), New Delhi, 2019

MODELLING OF NANOSTRUCTURES USING SECOND-ORDER STRAIN GRADIENT NONLOCAL THEORY

by

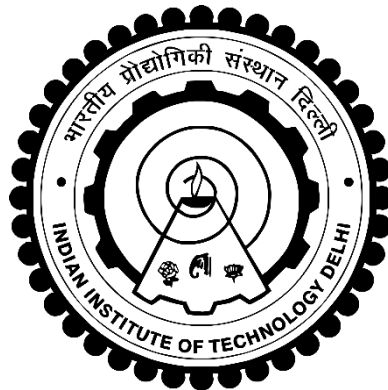
BISHWESHWAR BABU

Department of Applied Mechanics

Submitted

in fulfillment of the requirements of the degree of Doctor of Philosophy

to the



**INDIAN INSTITUTE OF TECHNOLOGY DELHI
AUGUST 2019**

Certificate

This is to certify that the thesis entitled “**Modelling of Nanostructures Using Second-Order Strain Gradient Nonlocal Theory**” being submitted by **Mr. Bishweshwar Babu** to the Indian Institute of Technology Delhi for the award of degree of **Doctor of Philosophy** in Applied Mechanics is a record of original, bonafide record of research work carried out by him under my supervision and guidance. The thesis work, in my opinion, has reached the requisite standard fulfilling the requirements for the degree of Doctor of Philosophy.

The results contained in this thesis have not been submitted in part or in full, to any other university or institute for the award of any degree or diploma.

Date: August , 2019

(B. P. Patel)

Place: New Delhi

Professor, Department of Applied Mechanics

Indian Institute of Technology Delhi

New Delhi, 110016, India

Acknowledgements

The real spirit of achieving a goal is through the way of excellence and strict discipline. I would have never succeeded in completing my task without the cooperation, encouragement and help from various personalities. Hence, the successful completion of this mammoth task would be incomplete without mentioning those who made it possible.

At first, I avail the opportunity to express my profound sense of indebtedness and gratitude to my respected supervisor Prof. B. P. Patel, Department of Applied Mechanics, Indian Institute of Technology Delhi for his inspiring guidance, encouragement, motivation, immense knowledge and invaluable help throughout the course of this work. Words are inadequate to express the great care and interest taken by him in all aspects of the present work, without which the work would not have reached its present form.

My appreciation and thanks are also expressed to my research committee members Prof. Suhail Ahmad, Prof. S. Pradyumna and Prof. S. P. Singh for their reviews, discussions and comments to improve the quality of the thesis. I would also like to express sincere thanks and gratitude to all the faculty members of Department of Applied Mechanics, Indian institute of Technology Delhi and Mr. V. S. Rawat, Jr. Technical Superintendent, Computation Laboratory for their kind help and support.

Sincere thanks are due to my friends and fellow research scholars of the Department of Applied Mechanics, Indian Institute of Technology Delhi, namely Anuj, Sandeep, Pritanshu, Rishav, Ajay, Arshad, Jitendra, Aswani, Gaurav, Adnan, Anurag, Mohit, Gargi, Amit, Mehnaz, Hamid, Lakhvinder, Shrish, Bashir, Sriram, Hasan, Vishwanath, Shivdayal, Shreya, Emarti, Sajan, Yadwinder, Ankita, Rishabh, Mayank

and Sumit for their wonderful company, for the stimulating discussions, for the sleepless nights we were working together, and for all the fun we have had which made my stay at Indian Institute of Technology Delhi, New Delhi very enjoyable and left me with an enriching experience for lifetime.

Finally, I want to express my gratitude from the inner soul of my heart to my mother Mrs. Bilasini Tripathy, my father Mr. Gyana Ranjan Babu, my sister Ms. Shwetapadma Babu and my grandmother Mrs. Shakuntala Babu for shaping my career, for their endless love, continuous encouragement, moral support and blessing to complete the work smoothly. They endured all the sufferings silently and looked forward to this day.

(Bishweshwar Babu)

Abstract

Modified continuum theories are needed to capture the size effects at micro/nano scale which are not accounted for by the classical theories in the absence of any internal length scale parameter. It is concluded from the literature review that the second-order strain gradient theories include only one nonlocal parameter and are capable of representing consistent nonlocal effect for different loading/boundary conditions. Analytical solutions for nonlocal beams/plates with different boundary conditions incorporating the strain gradient effect are not available in the literature. Further, there is a need to develop computationally efficient finite element formulations for the analyses of strain gradient nanobeams and nanoplates. The present work deals with the investigation of the static, stability and dynamic characteristics of nanobeams and nanoplates undergoing infinitesimal/finite deformation using the second-order strain gradient nonlocal theories.

The governing equations and the corresponding boundary conditions are derived for linear elastic isotropic Euler-Bernoulli beam with second-order positive and negative strain gradients based on Hamilton's principle. The variational statement with C^1 continuity requirement leads to unsymmetric nonlocal terms whereas the symmetrisation of the nonlocal terms leads to C^2 continuity requirement with additional boundary conditions. Analytical solutions for static bending, buckling and free vibration analyses are also derived to validate the finite element models. Results from the C^2 continuous model are found to be in excellent agreement with those from the analytical study. The second-order strain gradient model with negative nonlocal coefficient predicts physically meaningful results matching with the experimental investigations.

The governing equation and the corresponding classical/non-classical boundary conditions are derived for linear elastic isotropic Kirchhoff plate with second-order negative strain gradient term based on Hamilton's principle. Levy's analytical solution approach is extended for the analysis of static bending of rectangular strain gradient plates with different boundary conditions at the edges using the method of superposition. The weak form of the governing equation of motion requires C^2 continuity of transverse displacement. In the present work, a new computationally efficient 4-noded nonconforming rectangular finite element formulation with 6 degrees of freedom per node is presented. From static bending, buckling and free vibration analyses, this element is found to be computationally more efficient with better accuracy and convergence rate than the 4-noded C^2 continuous conforming element with 9 degrees of freedom per node.

The governing equation and the corresponding classical/non-classical boundary conditions are derived for geometrically nonlinear elastic isotropic Kirchhoff plate with second-order negative strain gradient term based on the principle of virtual work. The weak form requires C^1 continuity of the in-plane displacements and C^2 continuity of the transverse displacement. In the present work, a new computationally efficient 4-noded subparametric nonconforming finite element of arbitrary quadrilateral shape with 12 degrees of freedom per node is presented. The performance of the developed finite element is investigated for static bending of rectangular nanoplates involving five different combinations of clamped, simply supported and free edge boundary conditions.

From the detailed investigation, the effects of the positive and negative strain gradient terms are found to be of softening and hardening nature, respectively. Structures with geometry comparable to the microstructural length scale show significant size effect and this size dependency diminishes with the increase in the size of the structure.

सारांश

सूक्ष्म/अतिसूक्ष्म पैमाने पर आकार के प्रभावों को मापने के लिए संशोधित सातत्य सिद्धांतों की आवश्यकता होती है, जो कि किसी भी आंतरिक लंबाई पैमाने के मापदण्ड की अनुपस्थिति में पारम्परिक सातत्य सिद्धांतों के द्वारा संभव नहीं है। साहित्य समीक्षा से यह निष्कर्ष निकाला गया है कि द्वितीय कोटि के विकृति प्रवणता के सिद्धांतों में केवल एक गैर-स्थानीय मापदण्ड शामिल है और विभिन्न भारण/सीमा स्थितियों के लिए समनुरूप गैर-स्थानीय प्रभाव का प्रतिनिधित्व करने में सक्षम हैं। साहित्य में गैर-स्थानीय धरण/चादरों के लिए विकृति प्रवणता के प्रभाव को शामिल करने वाला विश्लेषणात्मक हल विभिन्न सीमा स्थितियों के साथ उपलब्ध नहीं हैं। इसके अलावा, विकृति प्रवण अतिसूक्ष्म धरण और अतिसूक्ष्म चादरों के विश्लेषण के लिए अभिकलनात्मक रूप से कुशल परिमित अल्पांश पद्धतियों को विकसित करने की आवश्यकता है। वर्तमान कार्य द्वितीय कोटि के विकृति प्रवणता के गैर-स्थानीय सिद्धांतों का उपयोग करते हुए बहुत छोटा/परिमित विस्थापन से गुजरने वाले अतिसूक्ष्म धरण और अतिसूक्ष्म चादरों की स्थैतिक, स्थिरता और गतिशील विशेषताओं की जांच से संबंधित है।

द्वितीय कोटि के सकारात्मक और नकारात्मक विकृति प्रवणता के साथ रैखिक लोचदार समानुवर्ती ओइलर-बर्नौली धरण के लिए हैमिल्टन के सिद्धांत पर आधारित संचालन समीकरण और संबंधित सीमा स्थितियां व्युत्पन्न की गयी हैं। सी-१ निरंतरता के आवश्यकता के साथ वाले विवरण कथन में असममित गैर-स्थानीय पद आते हैं जबकि गैर-स्थानीय पदों का सममितिकरण अतिरिक्त सीमा स्थितियों के साथ सी-२ निरंतरता की आवश्यकता की ओर ले जाता है। परिमित अल्पांश प्रतिरूप के प्रमाणीकरण के लिए स्थिर वक्रण, अस्थिरता और मुक्त कंपन विश्लेषण के विश्लेषणात्मक हल भी व्युत्पन्न किए गए हैं। सी-२ निरंतरता वाले परिमित अल्पांश प्रतिरूप के आकलन विश्लेषणात्मक हल के आकलन के साथ उत्कृष्ट समझौते में पाये गए हैं। नकारात्मक गैर-स्थानीय गुणांक के साथ द्वितीय कोटि का विकृति प्रवणता प्रतिरूप प्रयोगात्मक आकलनों के अनुरूप भौतिक रूप से सार्थक परिणाम देता है।

द्वितीय कोटि के नकारात्मक विकृति प्रवणता के साथ रैखिक लोचदार समानुवर्ती किरचॉफ चादर के लिए हैमिल्टन के सिद्धांत पर आधारित संचालन समीकरण और संबंधित पारम्परिक/गैर-पारम्परिक सीमा स्थितियां व्युत्पन्न की गयी हैं। अध्यारोपण के सिद्धांत का उपयोग करके किनारों पर विभिन्न सीमा स्थितियों के साथ आयताकार विकृति प्रवण चादरों के स्थिर वक्रण के विश्लेषण के लिए लेवी के विश्लेषणात्मक हल पद्धति को विस्तृत किया गया है। गति के संचालन समीकरण के शिथिल विवरण कथन में अनुप्रस्थ विस्थापन की सी-२ निरंतरता की आवश्यकता पायी गयी है। वर्तमान कार्य में, एक नये अभिकलनात्मक रूप से कुशल ४-आसंधि वाले गैर-अनुरूपित आयताकार परिमित अल्पांश का सूत्रीकरण ६ स्वतंत्रता चर प्रति आसंधि के साथ प्रस्तुत किया गया है। स्थिर वक्रण, अस्थिरता और मुक्त कंपन विश्लेषण के लिये यह अल्पांश बेहतर सटीकता और अभिसरण दर के साथ ९ स्वतंत्रता चर प्रति आसंधि वाले ४-आसंधि सी-२ निरंतर अनुरूप आयताकार अल्पांश की तुलना में अभिकलनात्मक रूप से अधिक कुशल पाया गया है।

द्वितीय कोटि के नकारात्मक विकृति प्रवणता के साथ ज्यामितीय रूप से अरेखीय लोचदार समानुवर्ती किरचॉफ चादर के लिए आभासी कार्य के सिद्धांत पर आधारित संचालन समीकरण और संबंधित पारम्परिक/गैर-पारम्परिक सीमा स्थितियां व्युत्पन्न की गयी हैं। शिथिल विवरण कथन में अनुदैर्घ्य विस्थापन की सी-१ निरंतरता और अनुप्रस्थ विस्थापन की सी-२ निरंतरता की आवश्यकता पायी गयी है। वर्तमान कार्य में, १२ स्वतंत्रता चर प्रति आसंधि वाले स्वेच्छित ढंग से चतुर्भुज के आकार के एक नये अभिकलनात्मक रूप से कुशल ४-आसंधि वाले उप-प्राचलिक गैर-अनुरूपित परिमित अल्पांश प्रस्तुत किया गया है। विकसित परिमित अल्पांश के प्रदर्शन की जांच आयताकार अतिसूक्ष्म चादरों के स्थिर वक्रण के लिए किया गया है, जिसमें पांच अलग-अलग सीमा स्थितियों के संयोजनों को शामिल किया गया है।

विस्तृत जांच से, सकारात्मक और नकारात्मक विकृति प्रवणता के प्रभाव क्रमशः नरम और सख्त प्रकृति के पाये गए हैं। सूक्ष्म संरचनात्मक लंबाई के पैमाने के साथ तुलनीय आकार की संरचनाएं महत्वपूर्ण आकार प्रभाव दिखाती हैं और संरचना के आकार में वृद्धि के साथ यह आकार निर्भरता कम हो जाती है।

Table of Contents

Certificate	i
Acknowledgements	iii
Abstract	v
Table of Contents	ix
List of Figures	xiii
List of Tables	xvii
Nomenclature and Abbreviations	xix
1. Introduction and Literature Review	1
1.1. Introduction	1
1.2. Eringen's Stress Gradient Theory	4
1.2.1. Beams	5
1.2.2. Plates	7
1.3. Higher-Order Strain Gradient and Inertia Gradient Theories	8
1.3.1. Second-Order Positive Strain Gradient Theory	8
1.3.2. Second-Order Negative Strain Gradient Theory	9
1.3.3. Fourth-Order Positive Strain Gradient Theory	11
1.3.4. Second-Order Positive/Negative Strain Gradient with Inertia Gradient Theory	11
1.3.5. Second-Order Hybrid Stress/Strain Gradient Theory	12
1.4. Modified Couple Stress Theory	14
1.4.1. Beams	15
1.4.2. Plates	16
1.5. Modified Strain Gradient Theory	17
1.5.1. Beams	19
1.5.2. Plates	20

1.6.	Mechanically Based Nonlocal Theory	21
1.7.	Estimation of Nonlocal Parameters	23
1.7.1.	Eringen's Theory	23
1.7.2.	Higher-Order Strain Gradient and Inertia Gradient Theories	24
1.7.2.1.	Second-Order Positive Strain Gradient Theory	24
1.7.2.2.	Second-Order Negative Strain Gradient Theory	25
1.7.2.3.	Second-Order Positive Strain Gradient with Inertia Gradient Theory	25
1.7.3.	Modified Couple Stress and Modified Strain Gradient Theories	26
1.8.	Motivation and Objectives	26
1.9.	Organization of the Thesis	29
2.	Finite Element Analysis of Second-Order Strain Gradient Beams	31
2.1.	Introduction	31
2.2.	Mathematical Formulation	31
2.2.1.	Second-Order Strain Gradient Nonlocal Models	32
2.2.2.	Finite Element Formulation with C^1 Continuity (FE1)	33
2.2.3.	Finite Element Formulation with C^2 Continuity (FE2)	36
2.2.4.	Boundary Conditions	39
2.2.5.	Analytical Solution-1	42
2.2.6.	Analytical Solution-2	42
2.2.6.1.	Bending	42
2.2.6.2.	Buckling	48
2.2.6.3.	Free Vibration	49
2.3.	Results and Discussion	50
2.3.1.	Validation	51
2.3.2.	Parametric Study	51
2.3.2.1.	Bending	51
2.3.2.2.	Buckling and Free Vibration	59
2.3.2.3.	Stress Distribution	62
2.4.	Concluding Remarks	63

3. Analytical Solutions for Static Bending of Second-Order Negative Strain Gradient Rectangular Plates	65
3.1. Introduction	65
3.2. Mathematical Formulation	65
3.2.1. Second-Order Strain Gradient Nonlocal Model	67
3.2.2. Analytical Solution	69
3.2.2.1. Rectangular plate with all edges simply supported (SSSS) and subjected to UDL	73
3.2.2.2. Rectangular plate with one pair of non-adjacent edges simply supported and the other pair clamped (SCSC) and subjected to UDL	74
3.2.2.3. Rectangular plate with one pair of non-adjacent edges simply supported and the other pair free (SFSF) and subjected to UDL	75
3.2.2.4. Rectangular plate with one pair of non-adjacent edges simply supported while the third edge is clamped and the fourth edge is free (SCSF) and subjected to UDL	77
3.2.2.5. Rectangular plate with all edges clamped (CCCC) and subjected to UDL	78
3.3. Results and Discussion	85
3.4. Concluding Remarks	93
4. Finite Element Analysis of Second-Order Negative Strain Gradient Rectangular Plates	95
4.1. Introduction	95
4.2. Mathematical Formulation	95
4.2.1. Conforming Finite Element Formulation	97
4.2.2. Nonconforming Finite Element Formulation	99
4.2.3. Boundary Conditions	103
4.3. Results and Discussion	104
4.4. Concluding Remarks	110

5. Static Bending of Geometrically Nonlinear Second-Order Negative Strain Gradient Rectangular Plates	111
5.1. Introduction	111
5.2. Mathematical Formulation	111
5.2.1. Second-Order Strain Gradient Nonlocal Model	112
5.2.2. Finite Element Formulation and Shape Functions	118
5.2.3. Boundary Conditions	124
5.3. Results and Discussion	125
5.3.1. Validation	126
5.3.2. Parametric Study	127
5.3.3. Results with Skewed and Distorted Meshes	133
5.4. Concluding Remarks	134
6. Conclusions and Future Scope	137
6.1. Summary of the Work Done	137
6.2. Conclusions from the Present Work	138
6.3. Scope for Future Research	139
References	141
Appendix-A	159
Appendix-B	163
Appendix-C	165
Appendix-D	169
List of Publications	171
About the Author	173

List of Figures

Figure 2.1	Beam geometry and coordinate system.	32
Figure 2.2	5-noded beam element.	34
Figure 2.3	2-noded beam element with 5 degrees of freedom at each node.	37
Figure 2.4	Tip load (Q) versus maximum transverse displacement (w_0) curve for micro cantilever beams with different thicknesses ($L/h = 10$).	51
Figure 2.5	Ratio of maximum transverse displacements with and without nonlocal effect (w_{nl}/w_l) versus nonlocal parameter (l) curves under UDL for different values of aspect ratio (L/D) for (a) SS, (b) CC, (c) CS and (d) CF nanobeams.	57
Figure 2.6	Nondimensional transverse displacement (\bar{w}) versus nondimensional axial coordinate (x/L) curves under UDL for different values of nonlocal parameter (l) for (a) SS, (b) CC, (c) CS and (d) CF nanobeams.	58
Figure 2.7	Nondimensional stress distribution (S_{xx}) versus nondimensional axial coordinate (x/L) curves under UDL for different values of nonlocal parameter (l) for (a) SS, (b) CC, (c) CS and (d) CF nanobeams (negative strain gradient theory).	62
Figure 3.1	Plate geometry and coordinate system.	65
Figure 3.2	Rectangular plate simply supported along $x = \pm a/2$.	70
Figure 3.3	SSSS rectangular plate.	73
Figure 3.4	SCSC rectangular plate.	74

Figure 3.5	SFSF rectangular plate.	75
Figure 3.6	SCSF rectangular plate.	77
Figure 3.7	CCCC rectangular plate.	78
Figure 3.8	Ratio of maximum transverse displacements with and without nonlocal effect (w_{nl}/w_l) versus normalized gradient coefficient $(l/a)^2$ curve for SSSS square plate.	86
Figure 3.9	Percentage reduction in central/maximum transverse displacement (Δ) versus nonlocal parameter (l) curves under uniformly distributed transverse load for different sizes of (a) SSSS, (b) SCSC, (c) SFSF, (d) SCSF and (e) CCCC nanoplates.	92
Figure 4.1	4-noded rectangular conforming/nonconforming element.	98
Figure 5.1	4-noded element in (a) physical and (b) natural coordinate space.	119
Figure 5.2	Comparison of the nondimensional transverse displacement (w/h) versus nondimensional point load (Fab/Eh^4) curve at the center of rectangular SSSS1 SLGS.	126
Figure 5.3	Nondimensional maximum transverse displacement (w/h) versus nondimensional uniformly distributed load ($1000qab/Eh^2$) curves for square (a) SSSS, (b) CCCC, (c) SCSC, (d) SFSF; and (e) SCSF SLGSs for different values of the nonlocal parameter (l) ($a = b = 10$ nm).	127
Figure 5.4	Nondimensional transverse displacement (w/h) vs nondimensional coordinates x/a and y/b along $y=0$ and $x=0$, respectively, under uniformly distributed load ($q = 1.5 \times 10^{-3}$ nN/nm ²) for different values of the nonlocal parameter (l) for square SSSS SLGS.	129

- Figure 5.5** Nondimensional transverse displacement (w/h) vs 130
nondimensional coordinates x/a and y/b along $y=0$ and
 $x=0$, respectively, under uniformly distributed load ($q =$
 3.9×10^{-3} nN/nm²) for different values of the nonlocal parameter
(l) for square CCCC SLGS.
- Figure 5.6** Nondimensional transverse displacement (w/h) along (a) $y=0$ 130
and (b) $x=0$ under uniformly distributed load ($q = 2.7 \times 10^{-3}$
nN/nm²) for different values of the nonlocal parameter (l) for
square SCSC SLGS.
- Figure 5.7** Nondimensional transverse displacement (w/h) along (a) 131
 $y = \pm b/2$ and (b) $x=0$ under uniformly distributed load ($q =$
 0.165×10^{-3} nN/nm²) for different values of the nonlocal
parameter (l) for square SFSF SLGS.
- Figure 5.8** Nondimensional transverse displacement (w/h) along (a) 131
 $y = -b/2$ and (b) $x=0$ under uniformly distributed load ($q =$
 0.3×10^{-3} nN/nm²) for different values of the nonlocal parameter
(l) for square SCSF SLGS.
- Figure 5.9** Nondimensional maximum transverse displacement (w/h) 132
versus nondimensional uniformly distributed load
($1000qab/Eh^2$) curves for rectangular (a) SSSS and (b) CCCC
SLGSs for different values of the nonlocal parameter (l) ($a =$
20 nm, $b = 10$ nm).
- Figure 5.10** Nondimensional maximum transverse displacement (w/h) 132
versus nondimensional uniformly distributed load
($1000qab/Eh^2$) curves for square (a) SSSS and (b) CCCC
SLGSs for different values of the nonlocal parameter (l) ($a = b$
 $= 20$ nm).

Figure 5.11 (a) Skewed mesh and (b) distorted mesh. 134

Figure 5.12 Nondimensional maximum transverse displacement (w/h) 134
versus nondimensional uniformly distributed load
($1000qab/Eh^2$) curves for square (a) SSSS and (b) CCCC
SLGSs using rectangular, skewed and distorted elements
($a = b = 10$ nm, $l = 0.5$ nm).

List of Tables

Table 2.1	Different sets of boundary conditions for SS Euler-Bernoulli beam.	40
Table 2.2	Different sets of boundary conditions for CC Euler-Bernoulli beam.	40
Table 2.3	Different sets of boundary conditions for CS Euler-Bernoulli beam.	41
Table 2.4	Different sets of boundary conditions for CF Euler-Bernoulli beam.	41
Table 2.5	Nondimensional maximum transverse displacement (\bar{w}) for SS Euler-Bernoulli nanobeam ($L/D = 10$).	53
Table 2.6	Nondimensional maximum transverse displacement (\bar{w}) for CC Euler-Bernoulli nanobeam ($L/D = 10$).	53
Table 2.7	Nondimensional maximum transverse displacement (\bar{w}) for CS Euler-Bernoulli nanobeam ($L/D = 10$).	54
Table 2.8	Nondimensional maximum transverse displacement (\bar{w}) for CF Euler-Bernoulli nanobeam ($L/D = 10$).	55
Table 2.9	Nondimensional critical buckling load (\bar{P}_c) for Euler-Bernoulli nanobeam ($L/D = 10$) from FE analysis.	60
Table 2.10	Nondimensional natural frequencies ($\bar{\omega}_m$) for Euler-Bernoulli nanobeam ($L/D = 10$) from FE analysis.	61
Table 3.1	Maximum displacements (w) and bending moments (M_{xx} and M_{yy}) under uniformly distributed transverse load for SSSS Kirchhoff nanoplate.	87

Table 3.2	Maximum displacements (w) and bending moments (M_{xx} and M_{yy}) under uniformly distributed transverse load for SCSC Kirchhoff nanoplate.	88
Table 3.3	Maximum displacements (w) and bending moments (M_{xx} and M_{yy}) under uniformly distributed transverse load for SFSF Kirchhoff nanoplate.	89
Table 3.4	Maximum displacements (w) and bending moments (M_{xx} and M_{yy}) under uniformly distributed transverse load for SCSF Kirchhoff nanoplate.	90
Table 3.5	Maximum displacements (w) and bending moments (M_{xx} and M_{yy}) under uniformly distributed transverse load for CCCC Kirchhoff nanoplate.	91
Table 4.1	Boundary conditions.	104
Table 4.2	Nondimensional values of maximum transverse displacement under uniformly distributed transverse load (\bar{w}) for SSSS, SCSC, SFSF, SCSF and CCCC Kirchhoff nanoplates.	106
Table 4.3	Nondimensional values of critical buckling load (\bar{P}_{cr}) for SSSS, SCSC, SFSF, SCSF and CCCC Kirchhoff nanoplates.	107
Table 4.4	Nondimensional values of fundamental natural frequency ($\bar{\omega}$) for SSSS, SCSC, SFSF, SCSF and CCCC Kirchhoff nanoplates.	108
Table 4.5	Comparison of computational time for conforming and nonconforming elements for static analysis of different boundary conditions.	109
Table 5.1	Boundary conditions.	124

Nomenclature and Abbreviations

English Notations

a, b	:	Dimensions of rectangular plate along x - and y -directions
a_e, b_e	:	Dimensions of rectangular element along x - and y -directions
a_0	:	Internal characteristic length
A, I	:	Area and second moment of area of beam cross section
\tilde{A}	:	Extensional rigidity
\mathbf{B}_e, \mathbf{B}	:	Elemental and global load vector due to the boundary integral terms
C_{ijkl}	:	Classical stiffness tensor
\mathbf{d}_i, \mathbf{d}	:	Nodal and global degrees of freedom vectors
$\mathbf{d}_e, \tilde{\mathbf{d}}_e$:	Elemental degrees of freedom vector
$\mathbf{d}_{u_0}, \mathbf{d}_{v_0}, \mathbf{d}_w$:	Elemental degrees of freedom vectors corresponding to u_0 , v_0 and w
$\mathbf{d}_{u_0i}, \mathbf{d}_{v_0i}, \mathbf{d}_{wi}$:	Nodal degrees of freedom vectors corresponding to u_0 , v_0 and w
$\delta_{u_0}, \delta_{v_0}, \delta_w$:	Elemental degrees of freedom vectors corresponding to u_0 , v_0 and w involving derivatives with respect to natural coordinates
$\delta_{u_0i}, \delta_{v_0i}, \delta_{wi}$:	Nodal degrees of freedom vectors corresponding to u_0 , v_0 and w involving derivatives with respect to natural coordinates
D	:	Diameter of the beam
\tilde{D}	:	Bending rigidity
E	:	Young's modulus
e_0	:	Material constant
e_{ijk}	:	Alternate tensor

f	:	Uniformly distributed axial load
F	:	Transverse point load at the center
\mathbf{F}_e, \mathbf{F}	:	Elemental and global load vectors
h	:	Thickness along z direction
$\mathbf{H}, \tilde{\mathbf{H}}, \mathbf{H}_w$:	Shape functions for w
$\mathbf{H}_{u_0}, \mathbf{H}_{v_0}$:	Shape functions for u_0 and v_0
$\bar{\mathbf{H}}_{u_0}, \bar{\mathbf{H}}_{v_0}, \bar{\mathbf{H}}_w$:	Shape functions for u_0, v_0 and w in natural coordinate space
I_0, I_0	:	Translatory and rotary inertia
$\mathbf{J}_1, \mathbf{J}_2, \mathbf{J}_3$:	First-, second- and third-order Jacobian transformation matrices
k	:	Wave number
\mathbf{K}_e, \mathbf{K}	:	Elemental and global stiffness matrices
$\mathbf{K}_{G_e}, \mathbf{K}_G$:	Elemental and global geometric stiffness matrices
l, l_0, l_1, l_2	:	Nonlocal parameters
l_m	:	Inertia related nonlocal parameter
L	:	Length of the beam
L_0	:	External characteristic length
L_e	:	Length of beam element
\mathbf{M}_e, \mathbf{M}	:	Elemental and global mass matrices
M_{xx}, M_{yy}, M_{xy}	:	Moment resultants about positive y - and negative x -axes, and twisting moment resultant about negative x -axis
n, s	:	Normal and tangential directions
\mathbf{N}	:	Shape functions for u_0
N_{xx}, P_{xx}	:	Boundary normal stress resultant and higher-order normal stress resultant on x -face
$\hat{N}_{xx}, \hat{P}_{xx}$:	Specified normal stress resultant and higher-order normal stress resultant on x -face
N_{xy}, P_{xy}	:	Boundary shear stress resultant and higher-order shear stress resultant on x -face

$\hat{N}_{xy}, \hat{P}_{xy}$:	Specified shear stress resultant and higher-order shear stress resultant on x -face
N_{yx}, P_{yx}	:	Boundary shear stress resultant and higher-order shear stress resultant on y -face
$\hat{N}_{yx}, \hat{P}_{yx}$:	Specified shear stress resultant and higher-order shear stress resultant on y -face
N_{yy}, P_{yy}	:	Boundary normal stress resultant and higher-order normal stress resultant on y -face
$\hat{N}_{yy}, \hat{P}_{yy}$:	Specified normal stress resultant and higher-order normal stress resultant on y -face
P_c	:	Critical buckling load
\bar{P}_c	:	Nondimensional critical buckling load
$\tilde{P}_{xx}, \tilde{P}_{yy}, \tilde{P}_{xy}$:	Applied in-plane compressive forces per unit length along x - and y -axes and applied in-plane shear force per unit length
q	:	Uniformly distributed transverse load
Q	:	Transverse tip load
r	:	Discrete particle radius
\mathbf{R}_e, \mathbf{R}	:	Elemental and global internal load vectors
S_{xx}	:	Nondimensional stress distribution
\mathbf{T}_e, \mathbf{T}	:	Elemental and global tangent stiffness matrices
T_{ij}	:	Classical stress tensor
u, v, w	:	Displacements along x -, y - and z -directions
u_0, v_0	:	Mid-plane displacements along x - and y -directions
$\hat{u}_0, \hat{v}_0, \hat{w}$:	Mid-plane displacements along x - and y -directions and transverse displacement specified at the boundaries
U	:	Strain energy
V	:	Volume occupied by the structure
$V_{xz}, \tilde{M}_{xx}, Q_{xx}$:	Boundary transverse shear stress resultant on x -face, moment resultant about y -axis and higher-order moment resultant about y -axis

$\hat{V}_{xz}, \hat{M}_{xx}, \hat{Q}_{xx}$:	Specified transverse shear stress resultant on x -face, moment resultant about y -axis and higher-order moment resultant about y -axis at $x = \pm a/2$
$V_{yz}, \tilde{M}_{yy}, Q_{yy}$:	Boundary transverse shear stress resultant on y -face, moment resultant about x -axis and higher-order moment resultant about x -axis
$\hat{V}_{yz}, \hat{M}_{yy}, \hat{Q}_{yy}$:	Specified transverse shear stress resultant on y -face, moment resultant about x -axis and higher-order moment resultant about x -axis at $y = \pm b/2$
\bar{w}	:	Nondimensional transverse displacement
w_c, w_p	:	Homogeneous solution and the particular integral
w_{nl}, w_l	:	Transverse displacements with and without nonlocal effect
x, y, z	:	Cartesian coordinates
x_e, y_e	:	Local element coordinates in physical coordinate space

Greek Notations

α	:	Nonlocal kernel
χ_{ij}^s	:	Symmetric rotation gradient tensor
δ_{ij}	:	Kronecker delta tensor
Δ	:	Percentage reduction in central/maximum transverse displacement
ε_{kl}	:	Classical strain tensor
$\varepsilon_{xx}, \varepsilon_{yy}, \gamma_{xy}$:	Normal strains in x - and y -directions and in-plane shear strain
ε_{xx}^0	:	Extensional strain
$\hat{\varepsilon}_{xx}, \hat{\gamma}_{xy}$:	Normal strain and shear strain specified at $x = \pm a/2$
$\hat{\varepsilon}_{yy}, \hat{\gamma}_{yx}$:	Normal strain and shear strain specified at $y = \pm b/2$
Γ	:	Boundary surrounding the structure
γ_i	:	Dilatation gradient vector
$\eta_{ijk}^{(1)}$:	Deviatoric stretch gradient tensor

κ_{xx}	:	Bending curvature
λ, μ	:	Lamé constants
ν	:	Poisson's ratio
$\hat{\theta}, \hat{\varepsilon}_0, \hat{\chi}$:	Slope, axial strain and curvature specified at the boundaries
$\hat{\theta}_x, \hat{\chi}_x$:	Slope about y-axis and curvature along x-axis specified at the boundaries $x = \pm a/2$
$\hat{\theta}_y, \hat{\chi}_y$:	Slope about x-axis and curvature along y-axis specified at the boundaries $y = \pm b/2$
ρ	:	Mass density
σ_{ij}	:	Nonlocal stress tensor
$\sigma_{xx}, \sigma_{yy}, \tau_{xy}$:	Normal stresses in x and y directions and in-plane shear stress
ω	:	Fundamental natural frequency
$\bar{\omega}$:	Nondimensional fundamental natural frequency
ω_m	:	Natural frequency of the m^{th} mode
$\bar{\omega}_m$:	Nondimensional natural frequency of the m^{th} mode
Ω	:	Surface area occupied by the structure
ξ, η	:	Natural coordinates
ψ	:	Compression ratio
∇^2	:	Laplacian operator

Abbreviations/Acronyms

AFM	:	Atomic Force Microscopy
AIREBO	:	Adaptive Intermolecular Reactive Empirical Bond Order
CC	:	Clamped-clamped
CCCC	:	All edges clamped
CF	:	Clamped-free/Cantilever
CNT	:	Carbon nanotube
CS	:	Clamped-simply supported/Propped cantilever
DLGS	:	Double-layered graphene sheet
DWCNT	:	Double-walled carbon nanotube

FDM	:	Finite Difference Method
FE1	:	Finite Element Formulation with C^1 Continuity
FE2	:	Finite Element Formulation with C^2 Continuity
FEM	:	Finite Element Method
MCST	:	Modified couple stress theory
MD	:	Molecular dynamics
MEMS	:	Micro-electro-mechanical systems
MLGS	:	Multi-layered graphene sheet
MSGT	:	Modified strain gradient theory
MWCNT	:	Multi-walled carbon nanotube
NEMS	:	Nano-electro-mechanical systems
SCSC	:	One pair of non-adjacent edges simply supported and the other pair clamped
SCSF	:	One pair of non-adjacent edges simply supported while the third edge clamped and the fourth edge free
SFSF	:	One pair of non-adjacent edges simply supported and the other pair free
SLGS	:	Single-layered graphene sheet
SS	:	Both ends simply supported
SSSS	:	All edges simply supported
SWCNT	:	Single-walled carbon nanotube
UDL	:	Uniformly distributed load